New Phytologist

Research

Metatranscriptomics reveals diversity of symbiotic interaction and mechanisms of carbon exchange in the marine cyanolichen *Lichina pygmaea*

Nathan Chrismas[1], Beth Tindall-Jones[1,2], Helen Jenkins[1], Joanna Harley[1], Kimberley Bird[1] and Michael Cunliffe[1,2]

[1]Marine Biological Association, The Laboratory, Citadel Hill, Plymouth, Devon, PL1 2PB, UK; [2]School of Biological and Marine Sciences, University of Plymouth, Plymouth, PL4 8AA, UK

Authors for correspondence:
Nathan Chrismas
Email: natchr@mba.ac.uk

Michael Cunliffe
Email: micnli@mba.ac.uk

Received: *21 July 2023*
Accepted: *21 September 2023*

New Phytologist (2023)
doi: 10.1111/nph.19320

Key words: carbon, Cyanobacteria, lichens, *Lichina pygmaea*, marine, symbiosis.

Summary

- Lichens are exemplar symbioses based upon carbon exchange between photobionts and their mycobiont hosts. Historically considered a two-way relationship, some lichen symbioses have been shown to contain multiple photobiont partners; however, the way in which these photobiont communities react to environmental change is poorly understood.
- *Lichina pygmaea* is a marine cyanolichen that inhabits rocky seashores where it is submerged in seawater during every tidal cycle. Recent work has indicated that *L. pygmaea* has a complex photobiont community including the cyanobionts *Rivularia* and *Pleurocapsa*. We performed rRNA-based metabarcoding and mRNA metatranscriptomics of the *L. pygmaea* holobiont at high and low tide to investigate community response to immersion in seawater.
- Carbon exchange in *L. pygmaea* is a dynamic process, influenced by both tidal cycle and the biology of the individual symbiotic components. The mycobiont and two cyanobiont partners exhibit distinct transcriptional responses to seawater hydration.
- Sugar-based compatible solutes produced by *Rivularia* and *Pleurocapsa* in response to seawater are a potential source of carbon to the mycobiont. We propose that extracellular processing of photobiont-derived polysaccharides is a fundamental step in carbon acquisition by *L. pygmaea* and is analogous to uptake of plant-derived carbon in ectomycorrhizal symbioses.

Introduction

While the original concept of symbiosis was built upon largely two-way relationships, it is now apparent that many symbioses are multipartner networks dominated by a few major players. Lichens are an archetype of symbiosis (Schwendener & Laue, 1869) that have been reinterpreted as complex communities (Hawksworth & Grube, 2020). Increased complexity in lichen symbiotic relationships has ecological and evolutionary implications. Multiple lineages of algae can coexist within a single thallus (Blaha *et al.*, 2006; Casano *et al.*, 2011), and locally adapted photobionts can improve survival of lichen fungi across changing environmental conditions (Ruprecht *et al.*, 2014; Werth & Sork, 2014).

Relationships with cyanobacterial photobionts (cyanobionts) make up *c.* 10% of lichen symbioses (Honegger, 2001). Despite the extensive diversity of the entire cyanobacterial phylum (Dvořák *et al.*, 2017), Cyanobacteria that are known to form lichen symbioses are largely in the Nostocales, with some representatives from other groups (Sanders & Masumoto, 2021). The primary role of Cyanobacteria in lichens varies. In cyanolichens, where Cyanobacteria are the primary photobiont, is that the cyanobiont is responsible for providing the mycobiont with the monosaccharide glucose for growth (Spribille *et al.*, 2022; Pichler *et al.*, 2023). In tripartite lichens, green algae provide sugar alcohols for growth while diazotrophic Cyanobacteria are mainly responsible for making fixed nitrogen available to the mycobiont (Feige, 1976; Brodo & Richardson, 1978) but may also contribute sugars (Henskens *et al.*, 2012).

In free-living Cyanobacteria, carbon metabolism has been relatively well-characterised (Herrero & Flores, 2008). In addition to glucose for use in respiration, free-living Cyanobacteria synthesise a variety of polymers including disaccharides (e.g. trehalose and sucrose) and sugar alcohols (e.g. glucosylglycerol), which are accumulated as compatible solutes under osmotic and desiccation stress (Reed & Stewart, 1983; Reed *et al.*, 1986; Asthana *et al.*, 2005; Sakamoto *et al.*, 2009; Klähn & Hagemann, 2011). The production of sugar-based compatible solutes is a survival mechanism for free-living Cyanobacteria in marine and brackish environments (Klähn & Hagemann, 2011). These simple sugars can later be exported from the cell alongside an array of complex extracellular polysaccharides (ExP) and other compounds as constituents of extracellular polymeric substances (EPS) (Pereira *et al.*, 2009, 2015; Chrismas *et al.*, 2016), which is also linked to salinity stress (Bemal & Anil, 2018). For Cyanobacteria in lichen symbioses, the established view is that only glucose is produced

and exchanged with the mycobiont (Spribille *et al.*, 2022; Pichler *et al.*, 2023) without consideration of other compounds made by free-living Cyanobacteria, despite the fact that genes involved in the direct export of glucose from cyanobacterial cells have not been identified (Stebegg *et al.*, 2019).

Lichina pygmaea (Lightf. C. Ag.) is a black cyanolichen found in the eulittoral zone of North Atlantic rocky shores (Naylor, 1930) (Fig. 1ai,aii). Marine lichens such as *L. pygmaea* survive in uniquely dynamic environments compared with terrestrial lichens (Tindall-Jones *et al.*, 2023) where exposure to desiccation and hydration (typically experienced by lichens) is combined with daily saltwater stress (Delmail *et al.*, 2013). In black fungi, adaptations to salinity stress include accumulation of sugars such as trehalose and mannitol, as well as production of mycosporines, mycosporine-like amino acids (MAAs), and melanin (Torres *et al.*, 2004; de la Coba *et al.*, 2009; Gostinčar *et al.*, 2012).

Recent DNA-based metabarcoding work has shown that the *L. pygmaea* photobiont community on southern UK shores contains two major cyanobacterial lineages: the filamentous diazotroph *Rivularia* (Nostocales) (Ortiz-Álvarez *et al.*, 2015; Chrismas *et al.*, 2021) and *Pleurocapsa* (Pleurocapsales) (Chrismas *et al.*, 2021), which appear intermingled in the lichen thallus (Fig. 1aiii). Pleurocapsales are not well known from terrestrial lichen symbioses (Jung *et al.*, 2021) but are associated with other marine lichens (Honegger, 2009).

Physical properties of carbon exchange in lichens have been explored experimentally, tracking transport of carbohydrates from photobiont to mycobiont (Honegger, 1991; Palmqvist, 2000). This transport is underpinned by molecular mechanisms of carbon uptake, export, and metabolism. While molecular aspects of interorganismal nutrient exchange have been explored in many symbiotic systems (e.g. corals; Shinzato *et al.*, 2014; Ryu *et al.*, 2019; arbuscular mycorrhizal fungi (AMF); Wang *et al.*, 2017; orchid mycorrhizal fungi; Valadares *et al.*, 2021; and ectomycorrhizal fungi (EMF); Rivera Pérez *et al.*, 2022), biological pathways of carbon exchange in lichens remain largely unknown (Pichler *et al.*, 2023). Progress in understanding molecular processes in lichens has been hampered in part by difficulty resynthesising *in vitro* a complete lichen thallus (Verma & Behera, 2015; Kono *et al.*, 2020; Spribille *et al.*, 2022) and scarcity of high-quality reference genomes for all partnered components of the symbiosis. The application of metatranscriptomics represents a tool for investigating gene expression and potential nutrient exchange pathways in nonmodel lichens *in natura*. So far, metatranscriptomics of lichens has focussed on the stress responses of lichen fungi (Junttila *et al.*, 2013; Wang *et al.*, 2015; Steinhäuser *et al.*, 2016; Chavarria-Pizarro *et al.*, 2022), photobionts (Steinhäuser *et al.*, 2016; Chavarria-Pizarro *et al.*, 2022), and the accessory microbiome (Cernava *et al.*, 2019) but has not yet been extensively used to examine the mechanisms of lichen symbiont interactions.

Understanding of photobiont diversity, responses to environmental change, and the fundamental mechanisms underpinning symbiotic interactions represent key knowledge gaps in our view of lichen biology. The combination of complex symbiosis (i.e. dominated by *L. pygmaea*, *Rivularia*, and *Pleurocapsa*) and exposure to regular major environmental change (i.e. frequent seawater coverage) makes *L. pygmaea* a suitable study system for exploring photobiont diversity and mechanisms of carbon exchange in relation to fluctuating environmental conditions. In this study, we use a combination of rRNA metabarcoding and mRNA metatranscriptomics to characterise diversity and symbiotic interactions within the *L. pygmaea* holobiont in response to rapid environmental change (i.e. seawater coverage). By using rRNA-based metabarcoding of the entire holobiont, we define the dominant organisms within the *L. pygmaea* microbial community in relation to previous DNA metabarcoding work (Chrismas *et al.*, 2021). We investigate the effect of the tidal cycle on mRNA relative abundance and compare the effects of hydration by seawater and rainwater across the entire holobiont. We use lineage-specific patterns of mRNA abundance to explore expression profiles of key cyanobacterial compatible solute biosynthesis and polysaccharide export genes typically studied in free-living Cyanobacteria but not previously explored in cyanobionts in lichen symbiosis. We propose candidate mechanisms of carbon exchange from photobiont to mycobiont, linking these processes to specific adaptations to survival in the marine environment. In doing so, we challenge existing general models of carbon exchange in lichen symbioses.

Materials and Methods

Lichina pygmaea sampling

Samples were collected from three individual thalli near the Marine Biological Association, Plymouth, UK (lat 50.363222, long −4.138833) (Fig. 1aii, Supporting Information Fig. S1) at high and low tide on 01/04/21 and 18/05/21 (12 samples in total, three from each of high and low tide on each date). On 01/04/21, the temperature at time of collection was 15°C with 62% humidity. An average of 0.74 mm precipitation had occurred in the preceding week. On 18/05/21, the temperature at time of collection was 11°C with 88% humidity. An average of 8.46 mm precipitation had occurred in the preceding week. On 01/04/21 at low tide, thalli were dry and brittle suggesting desiccation, whereas on 18/05/21 at low tide, thalli were noticeably hydrated. Upon collection, samples were cleaned to remove debris using sterile forceps. High tide samples (i.e. submerged in seawater) were washed with seawater. All samples were immediately flash frozen in liquid nitrogen and stored at −80°C.

RNA extraction

One hundred milligrams wet weight of lichen thallus was submerged in liquid nitrogen and ground to a powder using a pestle and mortar. Six hundred microlitres lysis buffer RLT was added to the powdered sample and mixed well by vortexing. Cell debris was removed by centrifuging at 9600 ***g*** for 30 s, the lysate was recovered, and an equal volume of 100% ethanol was added before being transferred to the RNeasy extraction column. RNA was then extracted following the manufacturer's protocol and included an on-column DNase digestion step using the

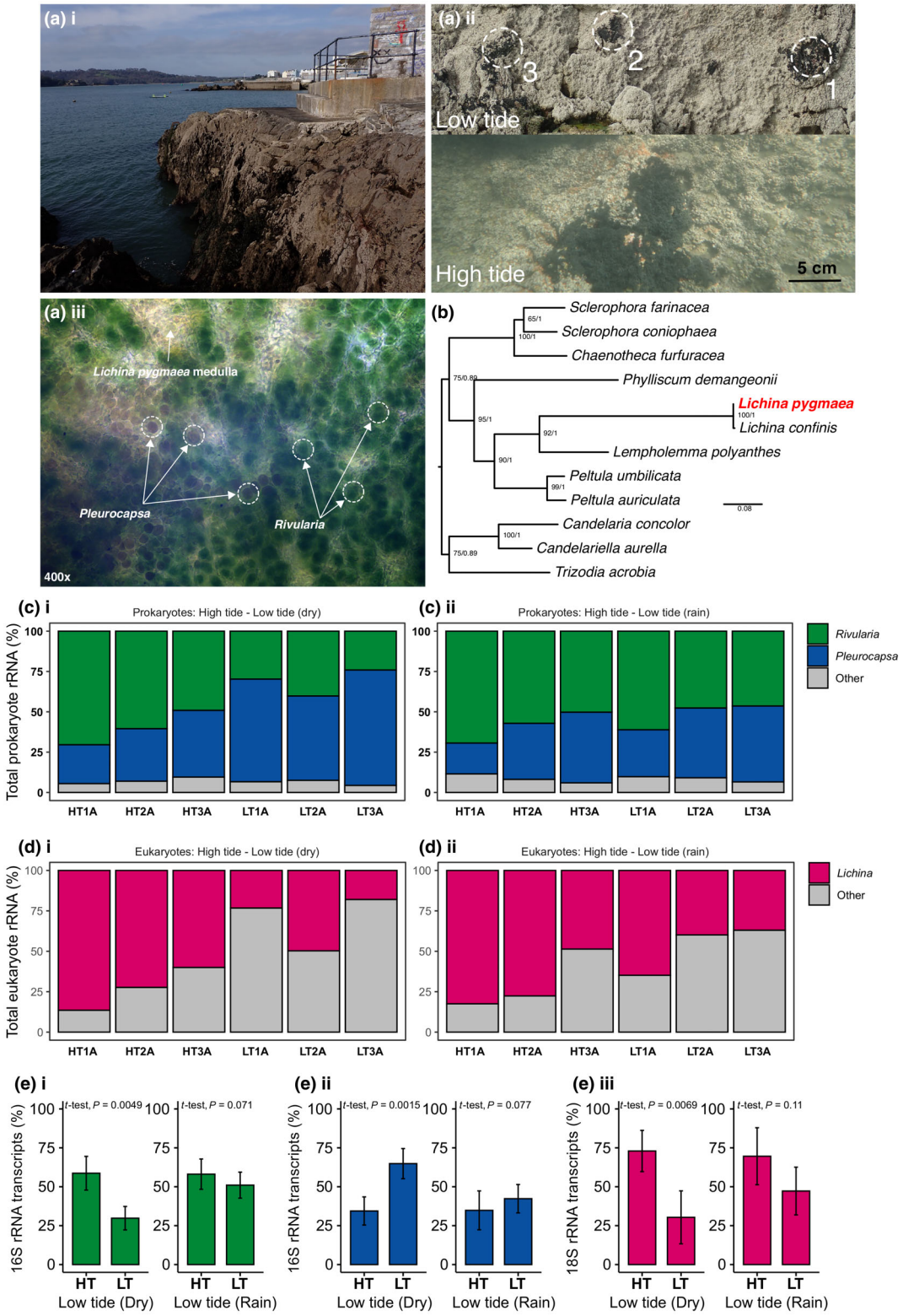

Fig. 1 (a) (i) *Lichina pygmaea* sample location in Plymouth. (ii) Individual thalli (circled) sampled at low tide and thallus 2 at high tide. (iii) Micrograph of *L. pygmaea* thallus with arrows indicating *L. pygmaea* medulla, and cells of *Rivularia* and *Pleurocapsa* (circled). *Rivularia* is visible as green cells and *Pleurocapsa* is visible as brown cells. (b) Multigene phylogeny (including *nuSSU*, *nuLSU*, *mtSSU* for *L. pygmaea* and *L. confinis* with additional *mcm7*, *RPB1*, and *RPB2* for other taxa from Prieto *et al*., 2019) of lichenised Lichinomycetes (*sensu* Díaz-Escandón *et al*., 2022) including *L. pygmaea* (Supporting Information Methods S1). Node labels indicate support from Maximum Likelihood (bootstraps) and Bayesian (posterior probabilities) trees, (c) 16S rRNA metabarcoding of bacteria associated with *L. pygmaea* at high tide and low tide when thallus was (i) dry at low tide and (ii) wet from rainwater at low tide. (d) 18S rRNA metabarcoding of eukaryotes associated with *L. pygmaea* at high tide and low tide when thallus was (i) dry at low tide and (ii) wet from rainwater at low tide. (e) differences in rRNA abundance between tidal states for (i) *Rivularia*, (ii) *Pleurocapsa*, and (iii) *Lichina*.

RNase-Free DNase set (Qiagen). RNA was quantified using the RNA BR assay kit (Invitrogen) on the Qubit 4 fluorometer (Invitrogen). RNA quality was assessed using the RNA 6000 Nano kit total RNA assay (Agilent) run on the 2100 Bioanalyzer instrument (Agilent, Stockport, Cheshire, UK) (Table S1). From 1 µg of RNA per sample, cDNA was produced using the Qiagen Omniscript® Reverse Transcription Kit with random hexamer primers (Promega) according to the manufacturer's protocol.

Bacteria 16S rRNA metabarcoding and total eukaryote 18S rRNA

DNA barcoding and phylogenetic methods are described in Methods S1; Figs S2 and S3 (Fig. 1b). For rRNA metabarcoding, the V4 region of the Bacteria/Archaea 16S rRNA gene was amplified from the cDNA using the primers 515F (5′-GTGY CAGCMGCCGCGGTAA-3′) and 806R (5′-GGACTACNV GGGTWTCTAAT-3′) (Earth microbiome project protocol; Ul-Hasan *et al.*, 2019). The V9 region of the eukaryote 18S rRNA gene was amplified from the cDNA using the primers 1891f (5′-GTACACACCGCCCGTC-3′) and EukBr (5′-TGATCCTTCT GCAGGTTCACCTAC-3′) (Earth microbiome project protocol; Ul-Hasan *et al.*, 2019). Amplicons were sequenced using Illumina technology. Raw metabarcoding reads are deposited in NCBI SRA under BioProject PRJNA955459 (16S) and BioProject PRJNA955655 (18S). Sequencing yielded 770 510 raw reads for 16S amplicons and 850 126 raw reads for 18S amplicons. Raw reads were processed in R 3.6.3 (R Core Team, 2020) using the DADA2 pipeline (Callahan *et al.*, 2016). Poor-quality reads were discarded leaving 561 391 16S reads and 631 584 18S reads. Assembled reads were clustered as amplicon sequence variants (ASVs) (Callahan *et al.*, 2017) resulting in a total of 517 16S ASVs and 1950 18S ASVs. Taxonomy was assigned using the SILVA 128 (Quast *et al.*, 2013) and PR2 (Guillou *et al.*, 2013) databases for 16S and 18S ASVs, respectively (Fig. 1c,d).

Metatranscriptomes

Sequencing of the metatranscriptome was carried out on the Illumina platform. Raw metatranscriptome reads are deposited in NCBI SRA under BioProject PRJNA955232. Assembly and annotation were carried out using a custom pipeline (Fig. S4). Raw reads were error corrected using rCorrector 1.0.4 (Song & Florea, 2015) and uncorrectable read pairs removed using the FilterUncorrectablePEfastq.py script. Remaining Illumina adapters and poor-quality sequences were removed using Trim Galore 0.6.7 (Martin, 2011) yielding between 20 185 022 and 31 251 705 reads per sample. Reads belonging to rRNA (SSU and LSU) were screened with SortMeRNA 4.3.4 (Kopylova *et al.*, 2012) using the SILVA (Quast *et al.*, 2013) default database. GC content analysis was performed in FastQC 0.11.9 (Andrews, 2010) and plotted with total count normalised (Evans *et al.*, 2018) per million reads. Since assembling reads improves taxonomic classification over that achieved by short reads alone (Shakya *et al.*, 2019; Tran & Phan, 2020), replicates were pooled and co-assembled using rnaSPADES 3.11.1 (Bushmanova *et al.*, 2019). Contigs < 200 bp were removed and remaining contigs clustered at 90% using Cd-hit-est 4.7 (Fu *et al.*, 2012) before open reading frames (ORFs) were predicted using TransDecoder 5.5.0. Longest ORFs output by TransDecoder 5.5.0 were further clustered at 80% using Cd-hit-est 4.7 before being indexed using Salmon 0.14.1 (Patro *et al.*, 2017) in mapping-based mode with all corrected reads quantified in transcripts per million (TPM). All ORFs with > 1 TPM were identified using custom BASH scripts and extracted using the subseq command in seqtk 1.3, and ORFs that did not appear in all samples were dropped leaving a final co-assembled metatranscriptome comprising a total of 25 391 unigenes.

Translated mRNA transcripts were annotated using InterProScan 5.55–88.0 (Paysan-Lafosse *et al.*, 2023) and by carrying out Diamond 0.9.22.123 (Buchfink *et al.*, 2015) blast searches against the NCBI nr database (accessed 11 April 2022). Taxonomies assigned using the taxonomizr 0.8 package in R 3.6.3 (R Core Team, 2020). Since no specific reference genomes for the investigated taxa were available, unigenes were split up based upon NCBI taxonomy into Ascomycota (to capture *L. pygmaea* genes) and Cyanobacteria, and this was further subdivided into Nostocales and Pleurocapsales (to capture *Rivularia* and *Pleurocapsa* genes). Since differences in transcription are inflated when reads from multiple taxa of different abundance are present, validated reads from each sample were mapped to each taxonomically classified subset of unigenes using Salmon 0.14 to obtain separate symbiont metatranscriptomes.

Cyanobacterial genes were identified using tBlastn with an e-value cut-off of 0.00001 and a minimum qcov hsp percentage of 0.75 to search proteins involved in key carbon import, export, and metabolic processes (photosynthesis; Stebegg *et al.*, 2019; sugar transporters; Stebegg *et al.*, 2019; Nieves-Morión *et al.*, 2020; compatible solute biosynthesis; Klähn & Hagemann, 2011; and EPS export; Chrismas *et al.*, 2016) against the *Rivularia* and *Pleurocapsa* metatranscriptomes. Where multiple query genes had the same hit, the hit was assigned to the query with the highest score. Identified genes were further checked through Blastx searches against the NCBI nr database removing spurious hits and hits with < 75% identity to any protein in GenBank. Full lists of all queries used are shown in Dataset S1. Fungal genes (glycoside hydrolases (GH); Chrismas & Cunliffe, 2020; sugar transporters (ST); Peng *et al.*, 2018; compatible solute biosynthesis (CS); Dijksterhuis & de Vries, 2006) were identified with Hmmer 3.2.1 (Finn *et al.*, 2011) using hmm profiles obtained from pfam.xfam.org. Full lists of all Pfams used are shown in Dataset S1. Cellular locations of predicted fungal proteins were predicted using DeepTMHMM 1.0.18 (Hallgren *et al.*, 2022) (Dataset S1). Predicted function of *L. pygmaea* sugar transporters was determined by comparing phylogenetic relationships with known sugar transporter reference sequences from Peng *et al.* (2018; Fig. S5). Sequences were aligned using Mafft 7.453 (Katoh & Standley, 2013) and phylogeny constructed using the Cipres (Miller *et al.*, 2011) implementation of RAxML-HPC 8.2 (Stamatakis, 2014) using PROTCAT and BLOSUM62 with automatic bootstrapping. To test for differential levels of expression between high and low tide, DESeq2 (Love *et al.*, 2014)

analysis was performed on raw reads for each of the three symbiont metatranscriptomes ($n = 3$; Fig. S6).

Results

Lichina pygmaea holobiont diversity

16S rRNA metabarcoding showed that Cyanobacteria dominate rRNA abundance in the bacterial component of the *L. pygmaea* holobiont (Fig. 1ci,cii), with *Rivularia* (Nostocales) and *Pleurocapsa* (Pleurocapsales) the major genera, made up of 2 and 26 ASVs, respectively. There was a switch between rRNA relative abundance in the dominant Cyanobacteria genera in the *L. pygmaea* holobiont between dry thalli at low tide dominated by *Pleurocapsa* (LT 52–72%; HT 24–41%; *t*-test, $P = 0.0015$) and the reciprocal thalli at high tide submerged in seawater dominated by *Rivularia* (LT 24–40%; HT 49–70%; *t*-test, $P = 0.0049$) (Fig. 1ei,eii). When the thalli were hydrated at low tide because of recent rainfall, the distinction between *Pleurocapsa* and *Rivularia* was less apparent (Fig. 1ei,eii).

Other bacteria (i.e. non-Cyanobacteria) accounted for ≤ 10% 16S rRNA relative abundance in the holobiont communities and were made up mainly of Gammaproteobacteria and Flavobacteria, groups that have been previously associated with the *L. pygmaea* microbiome in DNA-based studies (West *et al.*, 2018). The most dominant Flavobacterium ASV was attributed to the genus *Jejundonia*, which contains a single species, *J. soesokkakensis*, first isolated from the boundary between a freshwater and marine habitat (Park *et al.*, 2013). The most dominant Gammaproteobacterium was attributed to the genus *Granulosicoccus*, which contains species isolated from seawater (Baek *et al.*, 2014) and brown algae (Park *et al.*, 2014).

Eukaryote 18S rRNA metabarcoding showed the dominance of a single Ascomycota ASV (97–100% all Ascomycete reads in any single sample) (Fig. 1d) that shared 100% similarity with the aligned portion of *L. pygmaea* 18S rRNA gene. *Lichina pygmaea* dominated 18S rRNA sequences at high tide when the thalli were submerged with seawater and were less abundant at the reciprocal low tide when the thalli were dry (LT 13–44%; HT 53–83%; *t*-test, $P = 0.0069$) (Fig. 1eiii). As with *Pleurocapsa* and *Rivularia*, there was no difference between low and high tide when the thalli were hydrated with rainwater at low tide and submerged with seawater at high tide (*t*-test, $P > 0.05$) (Fig. 1eiii).

Non-Ascomycota eukaryotes accounted for between *c.* 10 and 75% 18S rRNA relative abundance in the holobiont communities depending on tide, and included diatoms (Bacillariophyta), ciliates (Oligohymenophera), and amoebae (Vannellida). Ulvophyceae (Chlorophyta) previously identified with DNA-based 18S rRNA gene metabarcoding of the *L. pygmaea* holobiont (Chrismas *et al.*, 2021) accounted for < 1% relative abundance of the 18S rRNA sequences in this study.

Lichina pygmaea holobiont metatranscriptome

A total of 25 391 unique genes were determined from the mRNA sequences and included in the analysis. Most unique genes were assigned to Cyanobacteria (11 106 genes, 43.74% total genes) and Ascomycota (8725 genes, 34.36% total genes) (Fig. 2ai). Within the Cyanobacteria, 5343 (48.1% cyanobacterial genes) were assigned to Pleurocapsales (*Pleurocapsa*) and 4384 (39.47% cyanobacterial genes) were assigned to Nostocales (*Rivularia*) (Fig. 2aii). The GC content of the cyanobacterial and fungal components of the metatranscriptome showed distinct signatures, with most predicted *Pleurocapsa* and *Rivularia* genes having a GC content of *c.* 30–50% and most *Lichina* genes having a GC content of *c.* 50–70% (Fig. 2b). With *Rivularia*, most genes were represented by a single copy, whereas multiple copies were detected in *Pleurocapsa*, usually with one dominant (Dataset S1).

Relative mRNA transcript abundance of the three main components for the holobiont (i.e. *Pleurocapsa*, *Rivularia*, and *Lichina*) within the metatranscriptome varied with tidal state (Fig. 2c–e). When the thallus was dry at low tide, mRNA for genes associated with *Pleurocapsa* was typically more abundant at low tide compared with high tide, whereas mRNA relative abundance of *Rivularia* genes varied less between tidal states. mRNA relative abundance of most *Lichina* genes were typically higher at high tide compared with low tide. When the thallus was hydrated at low tide due to precipitation in the preceding 24 h, differences in relative mRNA abundance between tidal states were diminished. For the subsequent comparison of specific genes, only samples obtained when the thallus was dry at low tide were used to focus on the impact of seawater coverage.

Cyanobacterial photosynthesis

mRNA sequences were identified for genes encoding several key components of the photosynthetic apparatus including photosystem I (*psaA*), photosystem II (*psbA*), phycobilisomes (*cpcA*/*cpeA*), and RuBisCo (*rbcL*) in both *Rivularia* (with the exception of *cpeA*) and *Pleurocapsa* (Fig. 3). Photosystem II (*psbA*) mRNA was particularly abundant in both genera. With *Rivularia*, the two dominant *psbA* genes showed no difference in assigned mRNA abundance between high tide and low tide collected thalli (Fig. 3). Conversely, within *Pleurocapsa*, mRNA assigned to the dominant photosystem I (*psbA*) gene was more abundant at low tide when the thalli was dry compared with high tide when submerged in seawater (DESeq2 $\log_2$FoldChange = 1.33, $P_{adj} \leq 0.001$) (Fig. 3).

Cyanobacterial compatible solute biosynthesis

mRNA sequences assigned to unique genes indicate activity of several genes encoding enzymes for the biosynthesis of compatible solutes: sucrose (*spsA*, *spp*; *Rivularia* and *Pleurocapsa*), trehalose (*treS*, *treY*, *treZ; Rivularia* and *Pleurocapsa*), glucosylglycerol (*ggpP*, *ggpS*; *Pleurocapsa* only), and mannitol (*mtdH*; *Rivularia* only) (Fig. 4ai,aii). Relative abundance of mRNA assigned to *Rivularia* trehalose biosynthesis genes was *c.* 10-fold higher than *Pleurocapsa*. Abundance of mRNA for one copy of the mannitol dehydrogenase gene *mtdH* was greater at high tide in *Rivularia* (DESeq2 $\log_2$FoldChange = 1.64, $P_{adj} \leq 0.001$). Three abundant homologs for the sucrose-phosphate synthase *spsA* were identified

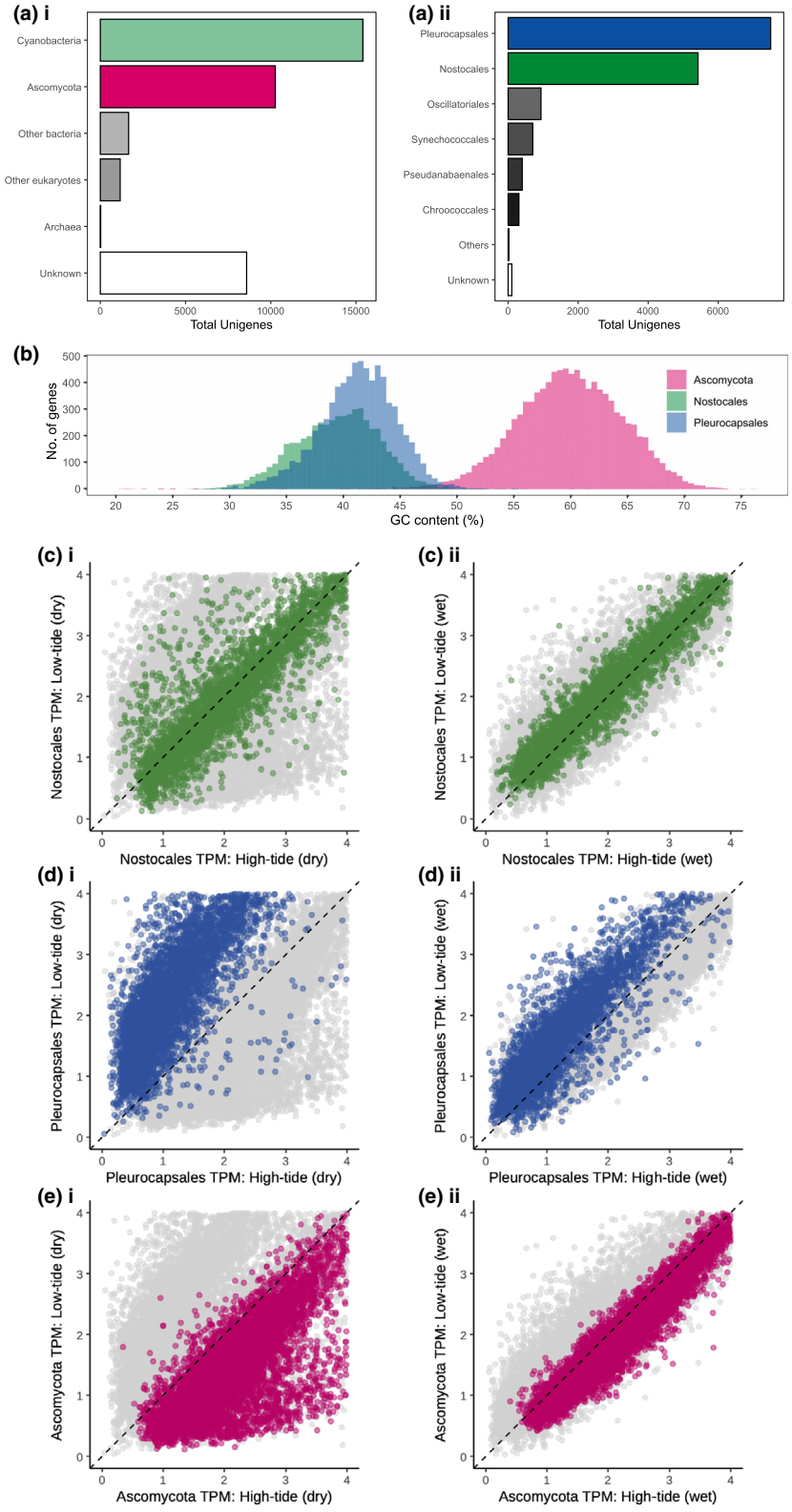

Fig. 2 Overview of the *Lichina pygmaea* holobiont metatranscriptome. (a) (i) Total numbers of unigenes assigned to Ascomycota, Cyanobacteria, and other taxonomic groups. (ii) Total numbers of unigenes assigned families of Cyanobacteria. (b) GC content of genes belonging to Ascomycota, Nostocales, and Pleurocapsales. (c, d) Total transcriptome mRNA abundance at high tide and low tide for Nostocales, Pleurocapsales, and Ascomycota when thallus was dry at low tide (ci, di, ei) and wet at low tide (cii, dii, eii). mRNA abundance for genes falling above the dashed lines is higher at low tide, mRNA abundance for genes falling below the dashed lines is higher at high tide.

in *Pleurocapsa*. Abundance of mRNA for these was greater at low tide (spsA.2 DESeq2 $\log_2$FoldChange = 2.82, $P_{adj} \leq 0.005$; spsA.3 DESeq2 $\log_2$FoldChange = 3.85, $P_{adj} \leq 0.001$; spsA.6 DESeq2 $\log_2$FoldChange = 1.14, $P_{adj} \leq 0.05$), although high levels of variance at low tide were observed for spsA.2 and spsA.3. There was a high abundance of mRNA for the glucosylglycerol-phosphate synthase gene *ggpS* in *Pleurocapsa*, which was greater at high tide (DESeq2 $\log_2$FoldChange = 0.79, $P_{adj} \leq 0.05$).

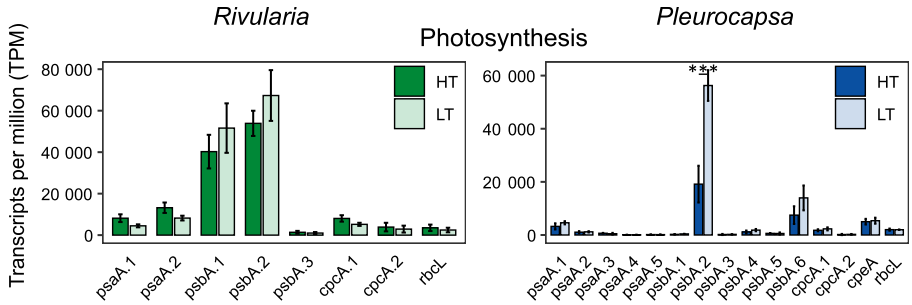

Fig. 3 Relative abundance of mRNA for cyanobacterial genes involved in photosynthesis in *Rivularia* and *Pleurocapsa* at high tide and low tide. Names indicate query gene/locus followed by a numerical indicator of copy detected within the metatranscriptome. Error bars represent standard deviation. Asterisks indicate DESeq2 significance: ***, $P_{adj} < 0.001$.

Cyanobacterial intracellular transport and export of organic carbon

Abundance of mRNA assigned to intracellular sugar transporters in *Rivularia* was low and with no differences between tidal states (Fig. 4bi). Abundance of mRNA for *Pleurocapsa* sugar transporters was more dynamic with two highly expressed copies of the sugar ATP-binding cassette (ABC) transporter ATP-binding gene all1823 occurring in at least one sample (Fig. 4bii). Abundance of mRNA assigned to both *Pleurocapsa* all18230.9 and all18230.14 was greater at low tide (all18230.9 DESeq2 $\log_2$FoldChange = 2.15, $P_{adj} \leq 0.001$; all18230.14 DESeq2 $\log_2$FoldChange = 1.037, $P_{adj} \leq 0.05$).

Extracellular polymeric substances export mechanisms in cyanobacteria are not fully understood, but several potential pathways have been identified (Pereira *et al.*, 2009, 2015). mRNA assigned to genes for predicted components of the Wzx-, ABC-transporter, and synthase dependent pathways of EPS export was identified within both the *Rivularia* and *Pleurocapsa* components of the metatranscriptome (Fig. 4c,d). In *Rivularia*, high abundance of mRNA was detected for two EPS-related genes in at least one treatment: the gene for the polysaccharide copolymerase (PCP) subunit of the wzx-dependent pathway (*wzc*) and the gene for the outer membrane polysaccharide export (OPX) subunit of the ABC-transporter dependent pathway (*kpsD*). mRNA for a copy of the *kpsT* ABC-transporter gene, kpsT.4, was more abundant at low tide ($\log_2$FoldChange = 2.24, $P_{adj} \leq 0.05$), as was a copy of the *wzx* gene wzx.3 ($\log_2$FoldChange = 1.72, $P_{adj} \leq 0.05$; Fig. 4ci). In *Pleurocapsa*, mRNA abundance for two genes was relatively high in at least one of high tide or low tide: mRNA for the OPX subunit of the ABC-transporter dependent pathway (*kpsD*) was more abundant during high tide (kpsD.1 $\log_2$FoldChange = 1.069, $P_{adj} \leq 0.005$) while mRNA for *kpsE* showed no difference between tidal states (Fig. 4cii).

Fungal glycoside hydrolases, sugar transporters, and compatible solute biosynthesis

The *L. pygmaea* metatranscriptome included 15 glycoside hydrolase families (Fig. 5a). mRNA for GH17 (predominantly endo-acting 1,3 β-glucosidases and licheninases) genes was highly abundant. mRNA for one extracellular GH65 (trehalase) was more abundant at high tide ($\log_2$FoldChange = 1.51, $P_{adj} \leq 0.001$). mRNA for several other glycoside hydrolases was present at lower levels. At high tide, mRNA was more abundant for GH3 (β-glucosidase) (GH3.1 $\log_2$FoldChange = 0.79, $P_{adj} < 0.05$; GH3.2 $\log_2$FoldChange = 0.97, $P_{adj} < 0.001$; GH3.3 $\log_2$FoldChange = 1.62, $P_{adj} \leq 0.001$) and GH16 (licheninase) (GH16.2 $\log_2$FoldChange = 1.45, $P_{adj} \leq 0.005$; GH16.3 $\log_2$FoldChange = −1.48, $P_{adj} \leq 0.005$). At low tide, mRNA was more abundant for a GH17 (licheninase) (GH17.2 $\log_2$FoldChange = 0.77, $P_{adj} \leq 0.005$) and a GH115 α-glucoronidase (GH115 $\log_2$FoldChange = 0.76, $P_{adj} \leq 0.05$).

mRNA for one transmembrane fungal sugar transporter, ST.1, was more abundant at high tide ($\log_2$FoldChange = 1.34, $P_{adj} \leq 0.001$) (Fig. 5b). Phylogenetic analysis placed this closest to known glucose transporters (Fig. S5). mRNA for one sugar transporter predicted to act on myoninositol (ST.4 $\log_2$FoldChange = 0.65, $P_{adj} \leq 0.05$) and one predicted to act on fructose (ST.6 $\log_2$FoldChange = 0.65, $P_{adj} \leq 0.005$) was significantly more abundant at low tide.

Fungal mRNA for genes related to trehalose biosynthesis (GT20, Trehalose phosphatase) was present at very low levels with no differences between tides (Fig. 5c). mRNA for fungal mannitol dehydrogenase (*mtdH*) was abundant at both high and low tide.

Discussion

Using rRNA metabarcoding and mRNA metatranscriptomics of the *L. pygmaea* holobiont, this study characterised the photobiont community and community level response to immersion in seawater as part of the tidal cycle. We show strong rRNA and mRNA signatures of two major cyanobiont lineages *Rivularia* and *Pleurocapsa*, alongside the *L. pygmaea* mycobiont. Each of the three major components of the holobiont display distinct responses to seawater hydration with important implications for the nature of the lichen symbiosis.

rRNA and transcriptional response supports complex cyanobiont diversity

While the very low abundance of Ulvophyceae in the rRNA metabarcoding suggests that green algae associated with

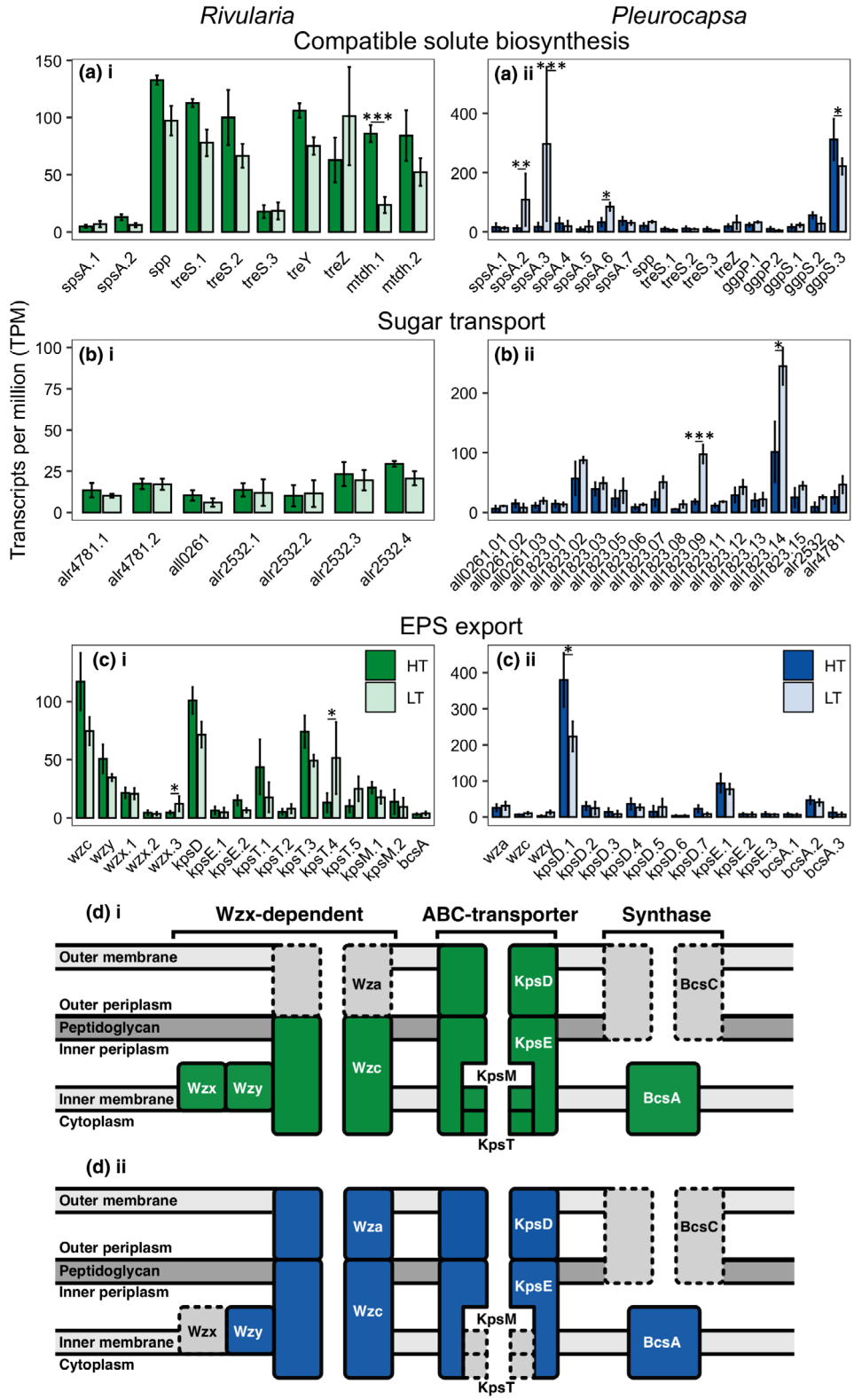

Fig. 4 Relative abundance of mRNA for cyanobacterial genes involved in (a) compatible solute biosynthesis, (b) sugar transport, and (c) Extracellular polymeric substance (EPS) export for *Rivularia* (ai–ci) and *Pleurocapsa* (aii–cii) at high tide and low tide. Names indicate query gene/locus followed by a numerical indicator of version detected within the metatranscriptome. Error bars represent standard deviation. Asterisks indicate DESeq2 significance: *, $P_{adj} < 0.05$; **, $P_{adj} < 0.005$; ***, $P_{adj} < 0.001$. (d) Schematic of EPS export mechanisms showing cellular architecture of key membrane transport proteins (after Pereira *et al*., 2015) for *Rivularia* (di) and *Pleurocapsa* (dii). Components with mRNA below detectable levels are shown in grey/dashed lines.

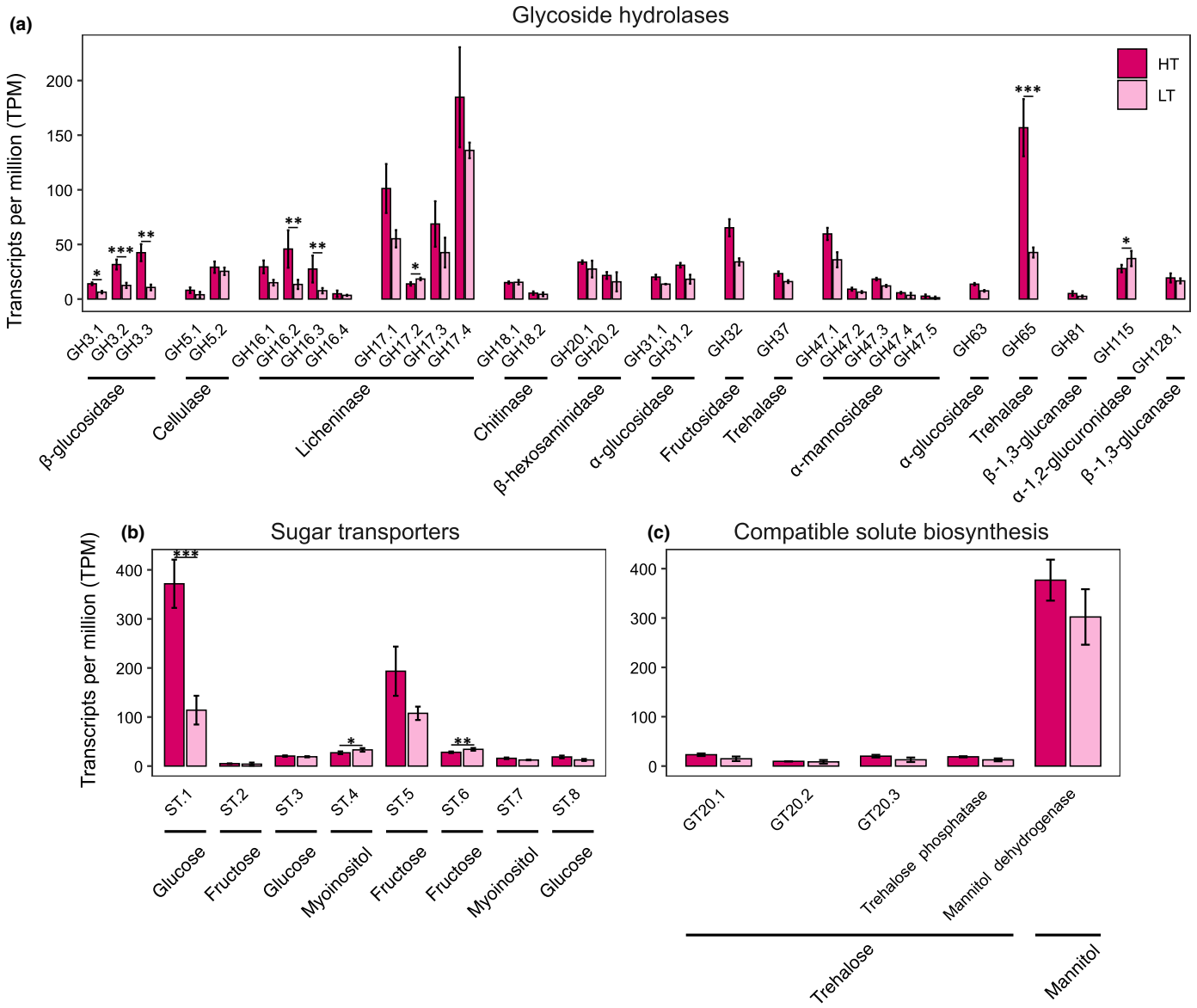

Fig. 5 Relative abundance of *Lichina pygmaea* mRNA for (a) glycoside hydrolases, (b) compatible solute biosynthesis genes and (c) sugar transporters at high and low tide. Names indicate query gene/locus followed by a numerical indicator of version detected within the metatranscriptome. Error bars represent standard deviation. Asterisks indicate DESeq2 significance: *, $P_{adj} < 0.05$; **, $P_{adj} < 0.005$; ***, $P_{adj} < 0.001$.

L. pygmaea (Chrismas *et al.*, 2021) do not represent a major active component of the symbiosis, our results show that *Pleurocapsa*, alongside *Rivularia*, is a major contributor to the overall abundance of transcribed rRNA genes. The presence of multiple *Pleurocapsa* ASVs in the rRNA data set and multiple copies of some *Pleurocapsa* genes in the mRNA data set corresponds well with previous indications of increased microdiversity of *Pleurocapsa* within a single *L. pygmaea* thallus relative to *Rivularia* (Chrismas *et al.*, 2021). The existence of photobiont diversity in the Lichinales has been reported elsewhere (Jung *et al.*, 2021), and Pleurocapsales have been identified as symbionts in marine lichens (LeCampion-Alsumard & Golubic, 1985), seaweeds (Bonthond *et al.*, 2021), and sponges (Konstantinou *et al.*, 2018) indicating a widespread importance of this group as symbionts in marine ecosystems. Further work is needed to better understand the full nature of these atypical lichen cyanobionts, and across co-occurring non-lichen intertidal taxa.

Hydration response varies between symbionts

The transcriptional response of the *L. pygmaea* mycobiont is consistent with poikilohydry, with increased rRNA and mRNA abundance occurring upon hydration, similar to terrestrial lichens (Kranner *et al.*, 2008; Cernava *et al.*, 2019). *Lichina pygmaea* rRNA and mRNA abundance increases in response to rainwater (like terrestrial lichens) as well as seawater, suggesting that *L. pygmaea* is tolerant of seawater rather than being halophilic.

The asymmetrical patterns of cyanobacterial rRNA and mRNA abundance suggest a degree of potential intralichen niche partitioning between cyanobionts, associated with the tidal cycle,

where *Rivularia* is dominant during high tide and *Pleurocapsa* is dominant at low tide. Raven *et al.* (1990) showed that *L. pygmaea* associated photosynthesis occurs throughout the tidal cycle. Our findings suggested that this activity could be divided alternately between *Rivularia* and *Pleurocapsa*, at least with *Pleurocapsa* more active at low tide. Although the dominant photobiont alternates between tidal states, photosynthetic activity in both *Pleurocapsa* and *Rivularia* as inferred by PSII mRNA abundance continues throughout. This has possible fitness implications for both mycobiont and photobionts as continuous photosynthesis during daylight hours irrespective of tidal state means a steady contribution to the available photobiont-derived C-pool that is then accessed by the mycobiont during high tide (discussed below). Moreover, since photobionts must satisfy their own nutritional requirements as well as those of the mycobiont, the ability to carry out photosynthesis when mycobiont activity is minimal during high tide may be key to balancing carbohydrate production and expenditure (Palmqvist, 2000).

For most genes, mRNA metatranscriptomics revealed similar patterns of activity to rRNA metabarcoding, although this differed in some specific genes suggesting a decoupling of general metabolic processes and other functional genes.

Cyanobiont compatible solutes/EPS as a source of carbon to the mycobiont

Production of compatible solutes is a key adaptive mechanism for free-living Cyanobacteria surviving in seawater (Klähn & Hagemann, 2011). In the case of *L. pygmaea*, compatible solute biosynthesis and export by *Rivularia* and *Pleurocapsa* may be critical to the overall function of the holobiont. In *Rivularia*, there was a high abundance of mRNA assigned to the key trehalose biosynthesis genes *treY* and *treZ*, presumably as part of a salinity tolerance mechanism as shown in free-living cyanobacteria (Klähn & Hagemann, 2011). Trehalose appears as a component of EPS, the export of which has also been linked to salinity adaptations in free-living Cyanobacteria (Bemal & Anil, 2018). Trehalose is a substrate for nonlichenised fungi (Jorge *et al.*, 1997; Jules *et al.*, 2004). When coupled with export via either the Wzc- or ABC-transporter dependent EPS export pathways, exogenous trehalose derived from *Rivularia* in response to seawater stress could be a source of organic carbon to *L. pygmaea*.

Although mRNA for trehalose biosynthesis genes was low abundance in *Pleurocapsa* in this study, a strong signal was seen for genes involved in biosynthesis of the compatible solutes glucosylglycerol and sucrose previously found in free-living Cyanobacteria (Klähn & Hagemann, 2011). mRNA abundance for the glucosylglycerol-phosphate synthase gene *ggpS* in *Pleurocapsa* shows a similar (but nonsignificant) pattern to trehalose biosynthesis genes in *Rivularia* and in some samples abundance of mRNA for the sucrose-6-phosphate synthase gene *spsA* in *Pleurocapsa* was particularly high during dry low tide (Fig. 4aii). In addition to synthesising sucrose as an osmolyte (Klähn & Hagemann, 2011), *spsA* is important in desiccation tolerance in free-living Cyanobacteria (Billi *et al.*, 2000), and this marked dehydration response may be important in allowing *Pleurocapsa* to function during low tide. The significant levels of mRNA for the putative EPS export gene *kpsD* at high tide in *Pleurocapsa* contrast with the overall expression pattern in this genus. This suggests a distinct response to tidal inundation, with potential for internal accumulation of osmolytes at low tide followed by export during high tide.

The production of trehalose (a disaccharide comprised of glucose) by *Rivularia* and sucrose (a disaccharide comprised of glucose and fructose) by *Pleurocapsa*, as proposed here through mRNA analysis, are supported by the original ^{14}C-based incubation experiments conducted by Smith (1968) to determine carbohydrates produced and released by *L. pygmaea* cyanobionts, which suggested that glucose (the widely considered cyanobiont carbon source for mycobionts; Spribille *et al.*, 2022; Pichler *et al.*, 2023) or glucosan (i.e. polysaccharides that yield glucose upon hydrolysis) is exchanged with the mycobiont (Smith, 1968).

While photobiont osmolytes are clearly available to the mycobiont, *L. pygmaea* appears able to produce osmolytes including trehalose (which may additionally be used for storage and transport; Deveau *et al.*, 2008; Ceccaroli *et al.*, 2011) and mannitol. While trehalose biosynthesis activity assigned to *L. pygmaea* was relatively low, expression of *mtdH* (the gene for the bidirectional mannitol dehydrogenase enzyme) was high (Fig. 5c), corresponding to previous observations of mannitol as an important osmolyte in *L. pygmaea* (Pueyo, 1963; Feige, 1972; Honegger *et al.*, 1993). Mannitol can be broken down by GH47 (also expressed, Fig. 5a) indicating the capacity for synthesis and recycling of mannitol within *L. pygmaea*, suggesting that *L. pygmaea* can produce its own osmolytes without needing to recycle them from the photobiont.

Exogenous glucose produced from trehalose and sucrose–a new carbon exchange pathway for cyanolichens?

In *L. pygmaea*, several mechanisms of carbon transfer from photobiont to mycobiont have been previously suggested. Feige (1972) proposed that glucose is passed directly across the photobiont/mycobiont contact zone, while Peveling (1973) suggested a vesicle-mediated exchange of metabolites based upon observations made using transmission electron microscopy (TEM). In the supralittoral sister species *Lichina confinis*, fungal haustoria were shown interacting with invaginations in cyanobacterial cells (Janson *et al.*, 1993). Regardless of the physical configuration of photobiont–mycobiont interactions, for cyanobiont-derived disaccharides such as trehalose and sucrose to be used by the mycobiont, an uptake mechanism is essential. In *L. pygmaea*, none of the identified sugar transporters clustered with those involved in direct uptake of extracellular trehalose (e.g. MAL11/AGT1; Stambuk *et al.*, 1998; Jules *et al.*, 2004). The same applies to sucrose transporters (e.g. SRT1; Wahl *et al.*, 2010). Instead, the fungal transmembrane sugar transporters that are most abundant in the mRNA cluster phylogenetically with glucose/fructose transporters (Fig. S5). Since *L. pygmaea* relies upon external carbon sources, this suggests that fungal hydrolysis of trehalose to glucose, and of sucrose to glucose and fructose, might occur extracellularly before uptake of resultant glucose monomers. The use of cyanobiont-derived trehalose as a carbon source by

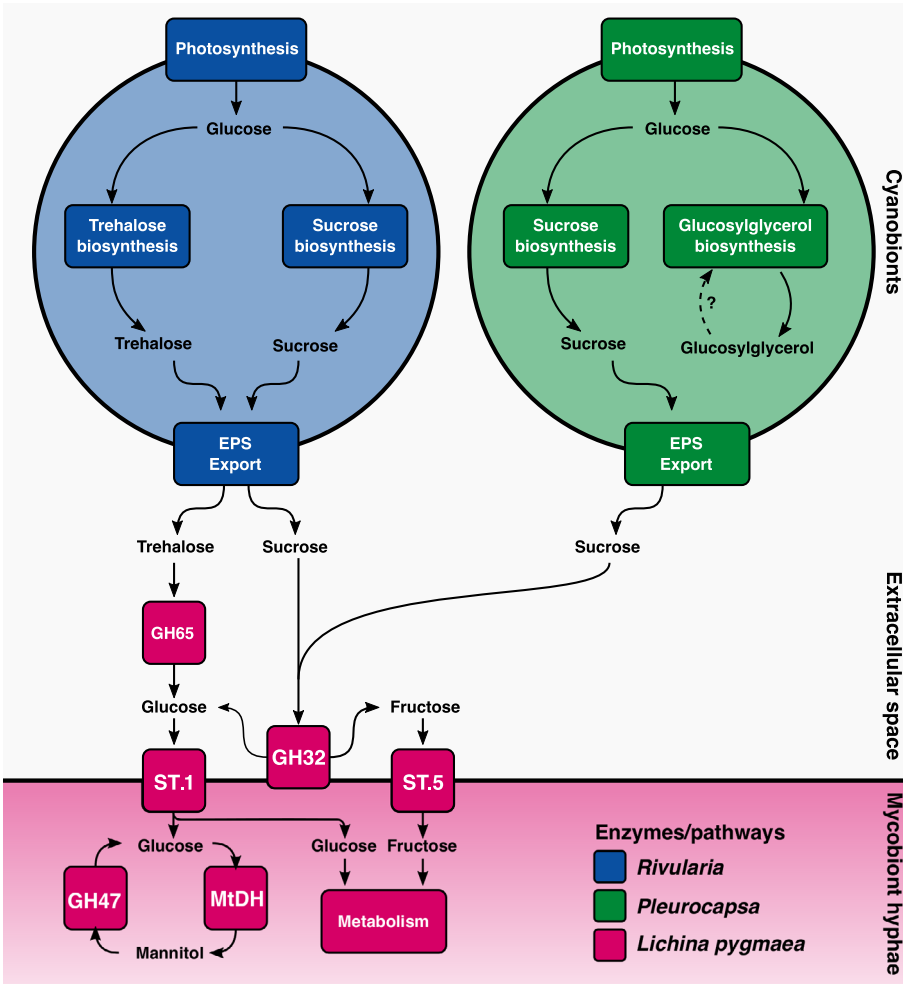

Fig. 6 Hypothetical pathways of carbohydrate exchange between *Rivularia*, *Pleurocapsa*, and *Lichina pygmaea*. Glucose derived from photosynthesis is synthesised into osmolytes trehalose and sucrose (*Rivularia*) or sucrose and glucosylglycerol (*Pleurocapsa*), which are used in salt and dehydration tolerance mechanisms. Carbohydrates are subsequently exported as components of extracellular polymeric substances (EPS) into the intrasymbiont space or else recycled. Exported carbohydrates are hydrolysed to their constituent monosaccharides by fungal extracellular enzymes (GH65/trehalose; GH32/sucrose) before uptake by specific sugar transporters (glucose/fructose). Once assimilated, sugars can then be used by *L. pygmaea* for metabolic processes and synthesis of osmolytes and storage compounds, that is mannitol. Dashed arrow indicates possible internal recycling of glucosylglycerol within *Pleurocapsa* via an unknown pathway.

L. pygmaea is supported by the high levels of expression of an extracellular acid trehalase (GH65) at high tide. Although neutral trehalases (GH37, also detected) are involved in processing internal trehalose as an osmolyte and storage compound, acid trehalases hydrolyse extracellular trehalose and have been described as 'carbon scavengers' that may allow fungi (e.g.*Saccharomyces cerevisiae*; Nwaka *et al.*, 1996; and *Mucor rouxii*; de Almeida *et al.*, 1997), to use exogenous trehalose as a source of carbon (Jorge *et al.*, 1997). A similar process could also apply to sucrose, which is hydrolysed to glucose and fructose by GH32 enzymes (Parrent *et al.*, 2009). A GH32 was detected in the metatranscriptome (Fig. 5a), as well as sugar transporters acting on fructose (Fig. 5b; Dataset S1) which, when combined with glucose transporters, provide a possible route for exogenous sucrose to be utilised by *L. pygmaea*. By contrast, there was no evidence for fungal GH13 activity, the main group of glycoside hydrolases acting on the compatible solute glucosylglycerol, suggesting that this may not be available as a substrate for *L. pygmaea* and may instead may be broken down to glucose and glycerol within *Pleurocapsa* by GgpS (Savakis *et al.*, 2016).

We propose that photobiont-derived carbon could be acquired by *L. pygmaea* in a mode analogous to carbon uptake by nonlichenised fungi, whereby disaccharides and polysaccharides are degraded to monosaccharides extracellularly before uptake and assimilation (i.e. Basidiomycetes; Rytioja *et al.*, 2014; Ascomycetes; De Vries *et al.*, 2000) (Fig. 6). Ectomycorrhizal fungi (ECM) lack polysaccharide transporters and hydrolyse plant-derived polysaccharides extracellularly before monosaccharides are taken up via monosaccharide transporters (Fajardo López *et al.*, 2008; Parrent *et al.*, 2009). The capacity to act on a wide diversity of carbohydrates appears to be common throughout lichens (Resl *et al.*, 2022), suggesting a range of potential substrates for lichen glycoside hydrolases. We show this activity may play a role in accessing a variety of carbohydrates directly from the photobiont. Similar utilisation of algal and cyanobacterial saccharides by black fungi may have been important in contributing to the evolution of a lichen lifestyle (Gostinčar *et al.*, 2012).

Conclusion

Photobiont biology underpins lichen symbiosis and understanding environmental responses of photobionts is essential to establish complete models of lichens. In *L. pygmaea*, the patterns of mRNA abundance in *Rivularia* and *Pleurocapsa* shown here reveal that environmental adaptation in the photobiont (i.e. response to inundation with seawater) may be fundamental to the overall functioning of the symbiosis. The inventory of expressed genes explored

here can be used to outline a model pathway for the assimilation of photobiont-derived carbohydrates by the fungus. In this proposed pathway, export of carbon is part of the cyanobiont stress response in a relatively atypical lichen habitat (i.e. the marine eulittoral zone) not normally considered. It is possible that alternative but related modes of glucose acquisition via exogenous hydrolysis occur in other cyanolichens as we have shown here in *L. pygmaea*. In future work, the use of other approaches such as TEM, immunolabelling and partnered genomes/metagenomes and transcriptomes will be useful in exploring further the nature of marine lichen mycobiont–photobiont relationships.

Acknowledgements

The authors wish to thank the anonymous referees for their comments and suggestions which greatly improved the manuscript. NC, KB and MC were supported by the European Research Council (ERC) project MYCO-CARB (grant no. 772584). HJ and JH were supported by the Wellcome Trust through the Darwin Tree of Life Discretionary Award (218328) and core funding to the Sanger Institute (206194).

Competing interests

None declared.

Author contributions

NC and MC conceived the study. NC, MC and BT-J carried out field sampling. JH carried out DNA barcoding. HJ constructed multigene phylogenies. BT-J and KB did the RNA extractions. NC performed rRNA metabarcoding analysis and assembled and analysed the metatranscriptome. NC and MC wrote the manuscript. All other authors commented on the manuscript.

ORCID

Kimberley Bird https://orcid.org/0000-0002-7244-5960
Nathan Chrismas https://orcid.org/0000-0002-2165-3102
Michael Cunliffe https://orcid.org/0000-0002-6716-3555
Joanna Harley https://orcid.org/0000-0003-3861-9127
Helen Jenkins https://orcid.org/0000-0003-1803-5183
Beth Tindall-Jones https://orcid.org/0000-0002-2898-0536

Data availability

RNA sequence data are available on NCBI under BioProjects PRJNA955459, PRJNA955655, and PRJNA955232. DNA barcodes are deposited in NCBI GenBank under accession nos. OR268985, OR268986, OR269923, OR269131, OR269132, and OR269922.

References

de Almeida FM, Lúcio AKB, De LTM PM, Jorge JA, Terenzi HF. 1997. Function and regulation of the acid and neutral trehalases of *Mucor rouxii*. *FEMS Microbiology Letters* **155**: 73–77.

Andrews S. 2010. FastQC: a quality control tool for high throughput sequence data. [WWW document] URL https://www.bioinformatics.babraham.ac.uk/projects/fastqc/ (accessed 14 March 2022).

Asthana RK, Srivastava S, Singh AP, Kayastha AM, Singh SP. 2005. Identification of maltooligosyltrehalose synthase and maltooligosyltrehalose trehalohydrolase enzymes catalysing trehalose biosynthesis in *Anabaena* 7120 exposed to NaCl stress. *Journal of Plant Physiology* **162**: 1030–1037.

Baek K, Choi A, Kang I, Im M, Cho J-C. 2014. *Granulosicoccus marinus* sp. nov., isolated from Antarctic seawater, and emended description of the genus *Granulosicoccus*. *International Journal of Systematic and Evolutionary Microbiology* **64**: 4103–4108.

Bemal S, Anil AC. 2018. Effects of salinity on cellular growth and exopolysaccharide production of freshwater *Synechococcus* strain CCAP1405. *Journal of Plankton Research* **40**: 46–58.

Billi D, Friedmann EI, Hofer KG, Caiola MG, Ocampo-Friedmann R. 2000. Ionizing-radiation resistance in the desiccation-tolerant cyanobacterium *Chroococcidiopsis*. *Applied and Environmental Microbiology* **66**: 1489–1492.

Blaha J, Baloch E, Grube M. 2006. High photobiont diversity associated with the euryoecious lichen-forming ascomycete *Lecanora rupicola* (Lecanoraceae, Ascomycota). *Biological Journal of the Linnean Society* **88**: 283–293.

Bonthond G, Shalygin S, Bayer T, Weinberger F. 2021. Draft genome and description of *Waterburya agarophytonicola* gen. nov. sp. nov. (Pleurocapsales, Cyanobacteria): a seaweed symbiont. *Antonie Van Leeuwenhoek* **114**: 2189–2203.

Brodo IM, Richardson DHS. 1978. Chimeroid associations in the genus peltigera. *The Lichenologist* **10**: 157–170.

Buchfink B, Xie C, Huson DH. 2015. Fast and sensitive protein alignment using Diamond. *Nature Methods* **12**: 59–60.

Bushmanova E, Antipov D, Lapidus A, Prjibelski AD. 2019. rnaSPADES: a *de novo* transcriptome assembler and its application to RNA-Seq data. *GigaScience* **8**: giz100.

Callahan BJ, McMurdie PJ, Holmes SP. 2017. Exact sequence variants should replace operational taxonomic units in marker-gene data analysis. *The ISME Journal* **11**: 2639–2643.

Callahan BJ, McMurdie PJ, Rosen MJ, Han AW, Johnson AJA, Holmes SP. 2016. DADA2: high-resolution sample inference from Illumina amplicon data. *Nature Methods* **13**: 581–583.

Casano LM, del Campo EM, García-Breijo FJ, Reig-Armiñana J, Gasulla F, del Hoyo A, Guéra A, Barreno E. 2011. Two *Trebouxia* algae with different physiological performances are ever-present in lichen thalli of *Ramalina farinacea*: coexistence versus competition? *Environmental Microbiology* **13**: 806–818.

Ceccaroli P, Buffalini M, Saltarelli R, Barbieri E, Polidori E, Ottonello S, Kohler A, Tisserant E, Martin F, Stocchi V. 2011. Genomic profiling of carbohydrate metabolism in the ectomycorrhizal fungus *Tuber melanosporum*. *New Phytologist* **189**: 751–764.

Cernava T, Aschenbrenner IA, Soh J, Sensen CW, Grube M, Berg G. 2019. Plasticity of a holobiont: desiccation induces fasting-like metabolism within the lichen microbiota. *The ISME Journal* **13**: 547–556.

Chavarria-Pizarro T, Resl P, Janjic A, Werth S. 2022. Gene expression responses to thermal shifts in the endangered lichen Lobaria pulmonaria. *Molecular Ecology* **31**: 839–858.

Chrismas NAM, Cunliffe M. 2020. Depth-dependent mycoplankton glycoside hydrolase gene activity in the open ocean-evidence from the Tara Oceans eukaryote metatranscriptomes. *The ISME Journal* **14**: 2361–2365.

Chrismas NAM, Allen R, Hollingsworth AL, Taylor JD, Cunliffe M. 2021. Complex photobiont diversity in the marine lichen *Lichina pygmaea*. *Journal of the Marine Biological Association of the United Kingdom* **101**: 667–674.

Chrismas NAM, Barker G, Anesio AM, Sanchez-Baracaldo P. 2016. Genomic mechanisms for cold tolerance and production of exopolysaccharides in the Arctic cyanobacterium *Phormidesmis priestleyi* BC1401. *BMC Genomics* **17**: 533.

de la Coba F, Aguilera J, Figueroa FL, de Gálvez MV, Herrera E. 2009. Antioxidant activity of mycosporine-like amino acids isolated from three red macroalgae and one marine lichen. *Journal of Applied Phycology* **21**: 161–169.

De Vries RP, Kester HC, Poulsen CH, Benen JA, Visser J. 2000. Synergy between enzymes from *Aspergillus* involved in the degradation of plant cell wall polysaccharides. *Carbohydrate Research* **327**: 401–410.

Delmail D, Grube M, Parrot D, Cook-Moreau J, Boustie J, Labrousse P, Tomasi S. 2013. Halotolerance in lichens: symbiotic coalition against salt stress. In: Ahmad P, Azooz MM, Prasad MNV, eds. *Ecophysiology and responses of plants under salt stress*. New York, NY, USA: Springer, 115–148.

Deveau A, Kohler A, Frey-Klett P, Martin F. 2008. The major pathways of carbohydrate metabolism in the ectomycorrhizal basidiomycete *Laccaria bicolor* S238N. *New Phytologist* **180**: 379–390.

Díaz-Escandón D, Tagirdzhanova G, Vanderpool D, Allen CCG, Aptroot A, Češka O, Hawksworth DL, Huereca A, Knudsen K, Kocourková J *et al.* 2022. Genome-level analyses resolve an ancient lineage of symbiotic ascomycetes. *Current Biology* **32**: 5209–5218.

Dijksterhuis J, de Vries RP. 2006. Compatible solutes and fungal development. *Biochemical Journal* **399**: e3.

Dvořák P, Casamatta DA, Hašler P, Jahodářová E, Norwich AR, Poulíčková A. 2017. Diversity of the cyanobacteria. In: Hallenbeck PC, ed. *Modern topics in the phototrophic prokaryotes: environmental and applied aspects*. Cham, Switzerland: Springer International Publishing, 3–46.

Evans C, Hardin J, Stoebel DM. 2018. Selecting between-sample RNA-Seq normalization methods from the perspective of their assumptions. *Briefings in Bioinformatics* **19**: 776–792.

Fajardo López M, Dietz S, Grunze N, Bloschies J, Weiß M, Nehls U. 2008. The sugar porter gene family of *Laccaria bicolor*: function in ectomycorrhizal symbiosis and soil-growing hyphae. *New Phytologist* **180**: 365–378.

Feige GB. 1972. Ecophysiological aspects of carbohydrate metabolism in the marine blue green algae lichen *Lichina pygmaea* AG. *Zeitschrift für Pflanzenphysiologie* **68**: 121–126.

Feige GB. 1976. Untersuchungen zur Physiologie der Cephalodien der Flechte *Peltigera aphthosa* (L) WILD. II. Das photosynthetische 14C-Markierungsmuster und der Kohlenhydrattransfer zwischen Phycobiot and Mycobiot Investigations on the Physiology of Cephalodia from the Lichen *Peltigera aphthosa*. *Zeitschrift für Pflanzenphysiologie* **80**: 386–394.

Finn RD, Clements J, Eddy SR. 2011. HMMER web server: interactive sequence similarity searching. *Nucleic Acids Research* **39**: W29–W37.

Fu L, Niu B, Zhu Z, Wu S, Li W. 2012. CD-HIT: accelerated for clustering the next-generation sequencing data. *Bioinformatics* **28**: 3150–3152.

Gostinčar C, Muggia L, Grube M. 2012. Polyextremotolerant black fungi: oligotrophism, adaptive potential, and a link to lichen symbioses. *Frontiers in Microbiology* **3**: 390.

Guillou L, Bachar D, Audic S, Bass D, Berney C, Bittner L, Boutte C, Burgaud G, de Vargas C, Decelle J *et al.* 2013. The Protist Ribosomal Reference database (PR2): a catalog of unicellular eukaryote small sub-unit rRNA sequences with curated taxonomy. *Nucleic Acids Research* **41**: 597–604.

Hallgren J, Tsirigos KD, Pedersen MD, Almagro Armenteros JJ, Marcatili P, Nielsen H, Krogh A, Winther O. 2022. DeepTMHMM predicts alpha and beta transmembrane proteins using deep neural networks. *bioRxiv*. doi: 10.1101/2022.04.08.487609.

Hawksworth DL, Grube M. 2020. Lichens redefined as complex ecosystems. *New Phytologist* **227**: 1281–1283.

Henskens FL, Green TGA, Wilkins A. 2012. Cyanolichens can have both cyanobacteria and green algae in a common layer as major contributors to photosynthesis. *Annals of Botany* **110**: 555–563.

Herrero A, Flores E. 2008. *The cyanobacteria: molecular biology, genomics and evolution*. Sevilla, Spain: Caister Academic Press.

Honegger R. 1991. Functional aspects of the lichen symbiosis. *Annual Review of Plant Physiology and Plant Molecular Biology* **42**: 553–578.

Honegger R. 2001. The symbiotic phenotype of lichen-forming ascomycetes. In: Hock B, ed. *The mycota: fungal associations*. Berlin, Heidelberg, Germany: Springer, 165–188.

Honegger R. 2009. Lichen-forming fungi and their photobionts. In: Deising HB, ed. *The mycota*. Berlin, Heidelberg, Germany: Springer, 307–333.

Honegger R, Kutasi V, Ruffner HP. 1993. Polyol patterns in eleven species of aposymbiotically cultured lichen mycobionts. *Mycological Research* **97**: 35–39.

Janson S, Rai AN, Bergman B. 1993. The marine lichen *Lichina confinis* (O. F. Müll.) C. Ag.: ultrastructure and localization of nitrogenase, glutamine synthetase, phycoerythrin and ribulose 1, 5-bisphosphate carboxylase/oxygenase in the cyanobiont. *New Phytologist* **124**: 149–160.

Jorge JA, Polizeli LTM, Thevelein JM, Terenzi HF. 1997. Trehalases and trehalose hydrolysis in fungi. *FEMS Microbiology Letters* **154**: 165–171.

Jules M, Guillou V, François J, Parrou J-L. 2004. Two distinct pathways for trehalose assimilation in the yeast *Saccharomyces cerevisiae*. *Applied and Environmental Microbiology* **70**: 2771–2778.

Jung P, Brust K, Schultz M, Büdel B, Donner A, Lakatos M. 2021. Opening the gap: rare lichens with rare cyanobionts – unexpected cyanobiont diversity in cyanobacterial lichens of the order lichinales. *Frontiers in Microbiology* **12**: 728378.

Junttila S, Laiho A, Gyenesei A, Rudd S. 2013. Whole transcriptome characterization of the effects of dehydration and rehydration on *Cladonia rangiferina*, the grey reindeer lichen. *BMC Genomics* **14**: 870.

Katoh K, Standley DM. 2013. MAFFT multiple sequence alignment software v.7: improvements in performance and usability. *Molecular Biology and Evolution* **30**: 772–780.

Klähn S, Hagemann M. 2011. Compatible solute biosynthesis in cyanobacteria. *Environmental Microbiology* **13**: 551–562.

Kono M, Kon Y, Ohmura Y, Satta Y, Terai Y. 2020. *In vitro* resynthesis of lichenization reveals the genetic background of symbiosis-specific fungal-algal interaction in *Usnea hakonensis*. *BMC Genomics* **21**: 671.

Konstantinou D, Gerovasileiou V, Voultsiadou E, Gkelis S. 2018. Sponges-cyanobacteria associations: global diversity overview and new data from the Eastern Mediterranean. *PLoS ONE* **13**: e0195001.

Kopylova E, Noé L, Touzet H. 2012. SortMeRNA: fast and accurate filtering of ribosomal RNAs in metatranscriptomic data. *Bioinformatics* **28**: 3211–3217.

Kranner I, Beckett R, Hochman A, Iii THN. 2008. Desiccation-tolerance in lichens: a review. *The Bryologist* **111**: 576–593.

LeCampion-Alsumard T, Golubic S. 1985. *Hyella caespitosa* Bornet et Flahault and *Hyella balani* Lehmann (Pleurocapsales, Cyanophyta): a comparative study. *Algological Studies/Archiv für Hydrobiologie* **38–39**: 119–148.

Love MI, Huber W, Anders S. 2014. Moderated estimation of fold change and dispersion for RNA-seq data with DESeq2. *Genome Biology* **15**: 550.

Martin M. 2011. Cutadapt removes adapter sequences from high-throughput sequencing reads. *EMBnet Journal* **17**: 10–12.

Miller MA, Pfeiffer W, Schwartz T. 2011. The Cipres science gateway: a community resource for phylogenetic analyses. In: *TG '11. Proceedings of the 2011 TeraGrid conference: extreme digital discovery*. New York, NY, USA: Association for Computing Machinery, 1–8.

Naylor GL. 1930. Note on the distribution of *Lichina confinis* and *L. pygmaea* in the Plymouth district. *Journal of the Marine Biological Association of the United Kingdom* **16**: 909–918.

Nieves-Morión M, Flores E, Foster RA. 2020. Predicting substrate exchange in marine diatom-heterocystous cyanobacteria symbioses. *Environmental Microbiology* **22**: 2027–2052.

Nwaka S, Mechler B, Holzer H. 1996. Deletion of the ATH1 gene in *Saccharomyces cerevisiae* prevents growth on trehalose. *FEBS Letters* **386**: 235–238.

Ortiz-Álvarez R, de los RA, Fernández-Mendoza F, Torralba-Burrial A, Pérez-Ortega S. 2015. Ecological specialization of two photobiont-specific maritime cyanolichen species of the Genus *Lichina*. *PLoS ONE* **10**: e0132718.

Palmqvist K. 2000. Tansley review no. 117 carbon economy in lichens. *New Phytologist* **148**: 11–36.

Park S, Jung Y-T, Won S-M, Park J-M, Yoon J-H. 2014. *Granulosicoccus undariae* sp. nov., a member of the family Granulosicoccaceae isolated from a brown algae reservoir and emended description of the genus *Granulosicoccus*. *Antonie Van Leeuwenhoek* **106**: 845–852.

Park S, Lee J-S, Lee K-C, Yoon J-H. 2013. Jejudonia soesokkakensis gen. nov., sp. nov., a member of the family Flavobacteriaceae isolated from the junction between the ocean and a freshwater spring, and emended description of the genus *Aureitalea* Park *et al.* 2012. *Antonie Van Leeuwenhoek* **104**: 139–147.

Parrent JL, James TY, Vasaitis R, Taylor AF. 2009. Friend or foe? Evolutionary history of glycoside hydrolase family 32 genes encoding for sucrolytic activity in fungi and its implications for plant-fungal symbioses. *BMC Evolutionary Biology* **9**: 148.

Patro R, Duggal G, Love MI, Irizarry RA, Kingsford C. 2017. Salmon provides fast and bias-aware quantification of transcript expression. *Nature Methods* **14**: 417–419.

Paysan-Lafosse T, Blum M, Chuguransky S, Grego T, Pinto BL, Salazar GA, Bileschi ML, Bork P, Bridge A, Colwell L *et al.* 2023. InterPro in 2022. *Nucleic Acids Research* **51**: D418–D427.

Peng M, Aguilar-Pontes MV, de Vries RP, Mäkelä MR. 2018. *In silico* analysis of putative sugar transporter genes in *Aspergillus Niger* using phylogeny and comparative transcriptomics. *Frontiers in Microbiology* **9**: 1045.

Pereira S, Zille A, Micheletti E, Moradas-Ferreira P, De Philippis R, Tamagnini P. 2009. Complexity of cyanobacterial exopolysaccharides: composition, structures, inducing factors and putative genes involved in their biosynthesis and assembly. *FEMS Microbiology Reviews* **33**: 917–941.

Pereira SB, Mota R, Vieira CP, Vieira J, Tamagnini P. 2015. Phylum-wide analysis of genes/proteins related to the last steps of assembly and export of extracellular polymeric substances (EPS) in cyanobacteria. *Scientific Reports* **5**: 14835.

Peveling E. 1973. Vesicles in the phycobiont sheath as possible transfer structures between the symbionts in the Lichen *Lichina Pygmaea*. *New Phytologist* **72**: 343–345.

Pichler G, Muggia L, Carniel FC, Grube M, Kranner I. 2023. How to build a lichen: from metabolite release to symbiotic interplay. *New Phytologist* **238**: 1362–1378.

Prieto M, Schultz M, Olariaga I, Wedin M. 2019. *Lichinodium* is a new lichenized lineage in the Leotiomycetes. *Fungal Diversity* **94**: 23–39.

Pueyo G. 1963. Un Polyalcool (Mannitol) Dans *Lichina pygmaea* Ag. *The Bryologist* **66**: 74–76.

Quast C, Pruesse E, Yilmaz P, Gerken J, Schweer T, Yarza P, Peplies J, Glöckner FO. 2013. The SILVA ribosomal RNA gene database project: improved data processing and web-based tools. *Nucleic Acids Research* **41**: D590–D596.

R Core Team. 2020. *R: a language and environment for statistical computing*. Vienna, Austria: R Foundation for Statistical Computing.

Raven JA, Johnston AM, Handley LL, McINROY SG. 1990. Transport and assimilation of inorganic carbon by *Lichina pygmaea* under emersed and submersed conditions. *New Phytologist* **114**: 407–417.

Reed RH, Borowitzka LJ, Mackay MA, Chudek JA, Foster R, Warr SRC, Moore DJ, Stewart WDP. 1986. Organic solute accumulation in osmotically stressed cyanobacteria. *FEMS Microbiology Letters* **39**: 51–56.

Reed RH, Stewart WDP. 1983. Physiological responses of *Rivularia Atra* to salinity: osmotic adjustment in hyposaline media. *New Phytologist* **95**: 595–603.

Resl P, Bujold AR, Tagirdzhanova G, Meidl P, Freire Rallo S, Kono M, Fernández-Brime S, Guðmundsson H, Andrésson ÓS, Muggia L *et al.* 2022. Large differences in carbohydrate degradation and transport potential among lichen fungal symbionts. *Nature Communications* **13**: 2634.

Rivera Pérez CA, Janz D, Schneider D, Daniel R, Polle A. 2022. Transcriptional landscape of ectomycorrhizal fungi and their host provides insight into N uptake from forest soil. *mSystems* **7**: e00957.

Ruprecht U, Brunauer G, Türk R. 2014. High photobiont diversity in the common European soil crust lichen *Psora decipiens*. *Biodiversity and Conservation* **23**: 1771–1785.

Rytioja J, Hildén K, Yuzon J, Hatakka A, de Vries RP, Mäkelä MR. 2014. Plant-polysaccharide-degrading enzymes from basidiomycetes. *Microbiology and Molecular Biology Reviews* **78**: 614–649.

Ryu T, Cho W, Yum S, Woo S. 2019. Holobiont transcriptome of colonial scleractinian coral *Alveopora japonica*. *Marine Genomics* **43**: 68–71.

Sakamoto T, Yoshida T, Arima H, Hatanaka Y, Takani Y, Tamaru Y. 2009. Accumulation of trehalose in response to desiccation and salt stress in the terrestrial cyanobacterium *Nostoc commune*. *Phycological Research* **57**: 66–73.

Sanders WB, Masumoto H. 2021. Lichen algae: the photosynthetic partners in lichen symbioses. *The Lichenologist* **53**: 347–393.

Savakis P, Tan X, Qiao C, Song K, Lu X, Hellingwerf KJ, Branco dos Santos F. 2016. Slr1670 from *Synechocystis* sp. PCC 6803 Is required for the re-assimilation of the osmolyte glucosylglycerol. *Frontiers in Microbiology* **7**: 1350.

Schwendener S, Laue C. 1869. *Die Algentypen der Flechtengonidien: Programm für Rectoratsfeier der Universitæt*. Basel, Switzerland: Universitætsbuchdruckerei von C. Schultze.

Shakya M, Lo C-C, Chain PSG. 2019. Advances and challenges in metatranscriptomic analysis. *Frontiers in Genetics* **10**: 904.

Shinzato C, Inoue M, Kusakabe M. 2014. A snapshot of a coral "Holobiont": a transcriptome assembly of the scleractinian coral, *porites*, captures a wide variety of genes from both the host and symbiotic zooxanthellae. *PLoS ONE* **9**: e85182.

Smith DC. 1968. The movement of carbohydrate from alga to fungus in lichens. *Bulletin de la Société Botanique de France* **115**: 129–133.

Song L, Florea L. 2015. rCorrector: efficient and accurate error correction for Illumina RNA-seq reads. *GigaScience* **4**: 48.

Spribille T, Resl P, Stanton DE, Tagirdzhanova G. 2022. Evolutionary biology of lichen symbioses. *New Phytologist* **234**: 1566–1582.

Stamatakis A. 2014. RAxML v.8: a tool for phylogenetic analysis and post-analysis of large phylogenies. *Bioinformatics* **30**: 1312–1313.

Stambuk BU, Panek AD, Crowe JH, Crowe LM, de Araujo PS. 1998. Expression of high-affinity trehalose–H^+ symport in *Saccharomyces cerevisiae*. *Biochimica et Biophysica Acta* **1379**: 118–128.

Stebegg R, Schmetterer G, Rompel A. 2019. Transport of organic substances through the cytoplasmic membrane of cyanobacteria. *Phytochemistry* **157**: 206–218.

Steinhäuser SS, Andrésson ÓS, Pálsson A, Werth S. 2016. Fungal and cyanobacterial gene expression in a lichen symbiosis: effect of temperature and location. *Fungal Biology* **120**: 1194–1208.

Tindall-Jones B, Cunliffe M, Chrismas N. 2023. Lichen zonation on UK rocky seashores: a trait-based approach to delineating marine and maritime lichens. *The Lichenologist* **55**: 91–99.

Torres A, Hochberg M, Pergament I, Smoum R, Niddam V, Dembitsky VM, Temina M, Dor I, Lev O, Srebnik M *et al.* 2004. A new UV-B absorbing mycosporine with photo protective activity from the lichenized ascomycete *Collema cristatum*. *European Journal of Biochemistry* **271**: 780–784.

Tran Q, Phan V. 2020. Assembling reads improves taxonomic classification of species. *Genes* **11**: 946.

Ul-Hasan S, Bowers RM, Figueroa-Montiel A, Licea-Navarro AF, Beman JM, Woyke T, Nobile CJ. 2019. Community ecology across bacteria, archaea and microbial eukaryotes in the sediment and seawater of coastal Puerto Nuevo, Baja California. *PLOS ONE* **14**: e0212355.

Valadares RBS, Marroni F, Sillo F, Oliveira RRM, Balestrini R, Perotto S. 2021. A transcriptomic approach provides insights on the mycorrhizal symbiosis of the mediterranean orchid *Limodorum abortivum* in nature. *Plants* **10**: 251.

Verma N, Behera BC. 2015. *In vitro* culture of lichen partners: need and implications. In: Upreti DK, Divakar PK, Shukla V, Bajpai R, eds. *Recent advances in lichenology: modern methods and approaches in lichen systematics and culture techniques, vol. 2*. Springer: New Delhi, India, 147–159.

Wahl R, Wippel K, Goos S, Kämper J, Sauer N. 2010. A novel high-affinity sucrose transporter is required for virulence of the plant pathogen *Ustilago maydis*. *PLoS Biology* **8**: e1000303.

Wang W, Shi J, Xie Q, Jiang Y, Yu N, Wang E. 2017. Nutrient exchange and regulation in arbuscular mycorrhizal symbiosis. *Molecular Plant* **10**: 1147–1158.

Wang Y, Zhang X, Zhou Q, Zhang X, Wei J. 2015. Comparative transcriptome analysis of the lichen-forming fungus *Endocarpon pusillum* elucidates its drought adaptation mechanisms. *Science China. Life Sciences* **58**: 89–100.

Werth S, Sork VL. 2014. Ecological specialization in Trebouxia (Trebouxiophyceae) photobionts of *Ramalina menziesii* (Ramalinaceae) across six range-covering ecoregions of western North America. *American Journal of Botany* **101**: 1127–1140.

West NJ, Parrot D, Fayet C, Grube M, Tomasi S, Suzuki MT. 2018. Marine cyanolichens from different littoral zones are associated with distinct bacterial communities. *PeerJ* **6**: e5208.

Supporting Information

Additional Supporting Information may be found online in the Supporting Information section at the end of the article.

Dataset S1 Gene identities, Blast Best Hits and DESeq2 results for all genes investigated in this study.

Fig. S1 Map indicating sampling location of *Lichina pygmaea* thalli.

Fig. S2 Bayesian phylogeny of lichenised Lichinomycetes.

Fig. S3 Maximum Likelihood phylogeny of lichenised Lichinomycetes.

Fig. S4 Step-by-step metatranscriptome assembly and annotation pipeline.

Fig. S5 Maximum Likelihood phylogeny of *Lichina pygmaea* sugar transporters.

Fig. S6 Volcano plots for *Rivularia* (green), *Pleurocapsa* (blue), and *Lichina pygmaea* (mauve).

Methods S1 *Lichina* spp. barcoding and multigene phylogeny.

Table S1 Agilent 2100 bioanalyzer results.

Please note: Wiley is not responsible for the content or functionality of any Supporting Information supplied by the authors. Any queries (other than missing material) should be directed to the *New Phytologist* Central Office.